Available online at www.sciencedirect.com
ScienceDirect
Tetrahedron 64 (2008) 1868–1878
Tetrahedron
www.elsevier.com/locate/tet

The influence of exocyclic phosphorous substituents on the intrinsic stability of four-membered heterophosphetes: a theoretical study

Zoltán Mucsi [a,*], István Hermecz [a], Béla Viskolcz [b], Imre G. Csizmadia [b], György Keglevich [a,*]

[a] Department of Organic Chemistry and Technology, Budapest University of Technology and Economics, H-1521 Budapest, Hungary
[b] Department of Chemistry and Chemical Informatics, Faculty of Education, University of Szeged, H-6725 Szeged, Hungary

Received 24 September 2007; received in revised form 21 November 2007; accepted 28 November 2007

Dedicated to Professor Csaba Szántay on his 80th birthday

Abstract

Four-membered heterophosphetes such as oxaphosphetes, thiaphosphetes, and azaphosphetes have long been considered desirable target molecules for organic chemists because of their interesting structural features. In spite of extensive investigation, only one azaphosphete and one thiaphosphete have been synthesized to date. In this paper, two possible conformers of these four-membered rings, as well as their open-ring phosphorane forms with a set of exocyclic substituents and a few ring heteroatoms were studied by molecular computations. The results suggested that the relative stability of these compounds is strongly dependent on the electronic effect of the exocyclic *P*-substituents. Three different types of exocyclic substituents X were recognized. However, only the strong electron-withdrawing substituents (X=F, CN, OCN, SCN) were able to stabilize the ring forms, providing the possibility to design stable heterophosphetes on the basis of the present computational results.

1. Introduction

In spite of nearly a century's effort—from Kekulé 1871 to Breslow and Dewar 1965—to synthesize cyclobutadiene, these attempts have proved to be unsuccessful.[1,2] Only theoretical chemistry was able to explain this failure by introducing the concept of antiaromaticity as a new phenomenon. The synthesis of these antiaromatic compounds has long been considered as desirable target of preparative chemistry in order to experimentally examine their strange chemical properties, but only a few compounds could be prepared and studied successfully. One of the examples may be the phosphole oxides and sulfides, which are proved to be antiaromatic phosphorous containing compounds.[3] Earlier studies[4] revealed that four-membered heterophosphetes (**1A** and **1B**) belong to the family of antiaromatic compounds and therefore cannot be isolated. This is in contrast to their saturated versions, the heterophosphetanes (**2**). Usually the corresponding cis (**3**) or trans (**3***) isomers of β-functionalized phosphoranes can be isolated,[5] rather than oxaphosphetes **1**. The overall process and structures may be summarized by Scheme 1. In principle, heterophosphetes (**1**) may adopt two distinct conformations.[4] The phosphorous–heteroatom bond (P1–Y2) can be either equatorial (**1A**) or apical (**1B**). The interconversion of the two forms falls into the domain of pseudorotation.[6,7] The strong conjugation between P1 and Y2 interacting with the C3=C4 double bond may result in certain antiaromatic character of **1**.[4] An equatorial Y2 can participate in a more extensive conjugation, therefore **1A** with an equatorial Y possesses stronger antiaromaticity, than **1B** having an apical Y2, which is rather non-conjugative.[4] In contrast to the ring-opening of **1**, an analogous ring-opening of **2** cannot be observed, as **4** does not represent a minimum on the potential energy surface (PES).[4] Only the two heterophosphetes (**5**,**6**) shown in Figure 1 have been reported in the literature as stable compounds.[8,9] According to X-ray crystallography,[8] the N···P distance in **5** is 2.170 Å, which is considerably longer than the sum of the covalent radii (1.06 Å+0.75 Å=1.81 Å).

* Corresponding authors. Tel.: +36 20 4416971; fax: +36 1 4633648.
E-mail address: zoltanmucsi@gmail.com (Z. Mucsi).

0040-4020/$ - see front matter © 2007 Elsevier Ltd. All rights reserved.
doi:10.1016/j.tet.2007.11.094

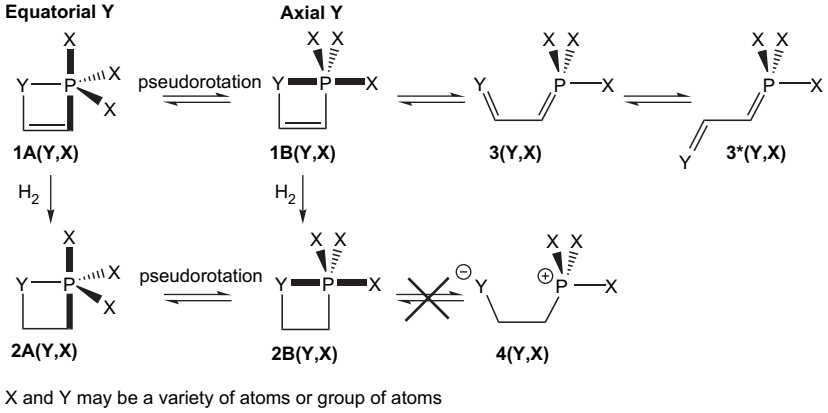

Scheme 1. Structural isomerization for heterophosphetes **1A** and **1B**, as well as heterophosphetanes **2A** and **2B**.

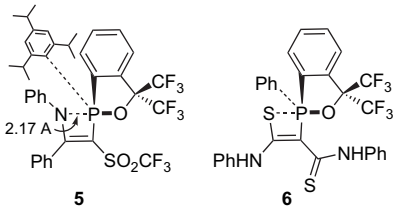

Figure 1. Prepared heterophosphetes (**5**,**6**).

Preliminary results suggested, however, that the chemical stability of **1** may be influenced by the electronic effect of the Y heteroatom and the exocyclic *P*-substituent (X).[4] In the present study, an intensive search has been carried out to find the proper combinations of Y and X that result in stable and isolatable **1**, in order to prepare and examine the physical and chemical properties of this compound.

The exact description of the aromatic or antiaromatic character of ring structures can be examined by different scales such as the HOMA index,[10] NICS values,[11,12] and enthalpies of isodesmotic reactions, resulting in an aromatic stabilizing energy (ASE).[13] The determination of the antiaromatic character of heterophosphete **1** is not simple by traditional means. HOMA index requires reference bond distances for completely aromatic and non-aromatic ring systems containing the same atoms in the ring. The NICS values show significant deviation from the usual values computed for carbocycles, which is due to the larger shielding effect of the large P atom combined with small ring size. It should be noted that the NICS(1) values are influenced by the exocyclic X substituents on P1 atom due to the steric proximity of the position X as well as the point 1 Å above the ring center. The results of homodesmic reactions may also be misleading, as the configuration around the P atom changes during the ring-opening reactions. A further possibility is that aromaticity and antiaromaticity are characterized by a common and universal linear scale based on the enthalpy of hydrogenation (see ΔH_{H2} and $\Delta\Delta H_{H2}$ in Fig. 2) when cyclobutadiene and benzene are considered as −100% and +100%, respectively.[14] This methodology compares the hydrogenation reaction of the examined compound [ΔH_{H2}(examined)] with that of a properly chosen reference reaction where an unsaturated analogue of the aromatic compound that does not possess any aromatic or antiaromatic character is also hydrogenated [ΔH_{H2}(ref.)] as shown in Figure 2.

The extent of antiaromaticity of **1A** and **1B** has been measured in terms of the following hydrogenation reactions (Eqs. 1–4)[14] depicted by Figure 2.[4]

$$\Delta H_{H2}(\text{exam.}) = H[\mathbf{2}(\mathbf{X},\mathbf{Y})] - \{H[\mathbf{1}(\mathbf{X},\mathbf{Y})] + H(H_2)\} \quad (1)$$

$$\Delta H_{H2}(\text{ref.}) = H[\mathbf{2}(\mathbf{X},\mathbf{CH_2})] - \{H[\mathbf{1}(\mathbf{X},\mathbf{CH_2})] + H(H_2)\} \quad (2)$$

$$\Delta\Delta H_{H2} = \Delta H_{H2}(\text{exam.}) - \Delta H_{H2}(\text{ref.}) \quad (3)$$

$$\text{Aromaticity} = m\Delta\Delta H_{H2} + b \quad (4)$$

where m=0.6844 and b=1.8637 at B3LYP/6-311++G(2d,2p) level of theory.[14]

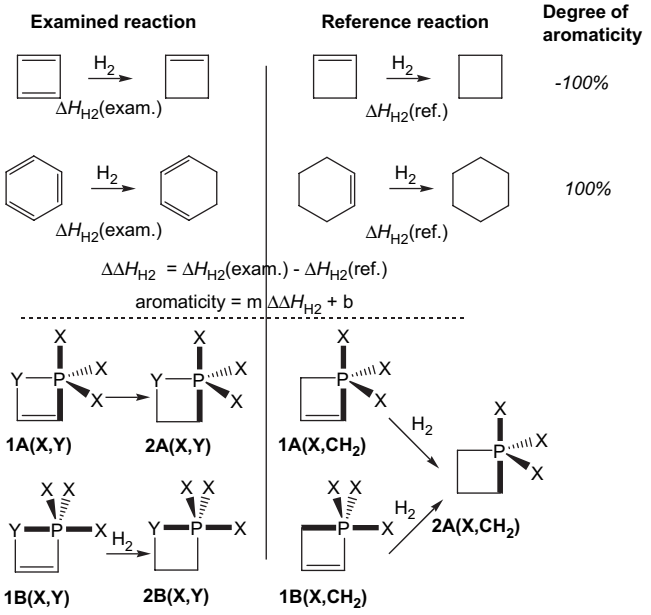

Figure 2. ΔH_{H2} values calculated for an antiaromatic and aromatic species. Note that **2A**(**X**,**CH$_2$**)≡**2B**(**X**,**CH$_2$**) are identical due to internal symmetry.

These equations are valid for both **A** and **B** conformers. It should be noted, however, that **2A(X,CH$_2$)** and **2B(X,CH$_2$)** are identical due to the internal symmetry. Previously the antiaromaticity values were determined for 3×3=9 heterophosphete congeners containing three ring heteroatoms (Y=NH, O, S) and three exocyclic substituents (X=F, Cl, CN) at B3LYP/6-311++G(2d,2p) level of theory,[4] indicating that their aromaticity values cover the area from −35% to +10%.

The present study aims to explore the effect of various structural features, such as electron-withdrawing (EWG) and electron-donating (EDG) substituents on the intrinsic stability of heterophosphetes. Both the kinetic (transition states, TS) and thermodynamic stabilities (Gibbs free energy differences, ΔG) are investigated for each X and Y to evaluate, which combination of substituents would stabilize **1A** or **1B** as possible synthetic targets. For this reason, three Y groups were used (NH, O, S) in combination with 12 X substituents, covering both electron-withdrawing (EWG: F, Cl, Br, CN, OCN, SCN, Ph) and electron-donating groups (EDG: OMe, SMe, NMe$_2$, Me) and H. One may propose putative energy profiles (Fig. 3) depending on the stabilizing and destabilizing effects of X and Y. The regular line (*Case I*) indicates a situation where the energy level of **3** is considerably lower than **1A** and **1B**. Consequently, heterophosphetes cannot be synthesized. The bold line (*Case II*) indicates a situation in which **1B** is lower on the energy scale than **3**; in this case, **1B** does not undergo ring opening to afford **3**, and therefore **1B** might be synthesized. In fact, one or both minima of heterophosphetes **1A** and **1B** could be annihilated on the PES due to unfavorable combinations of the substituents, and these structures therefore cannot be synthesized.

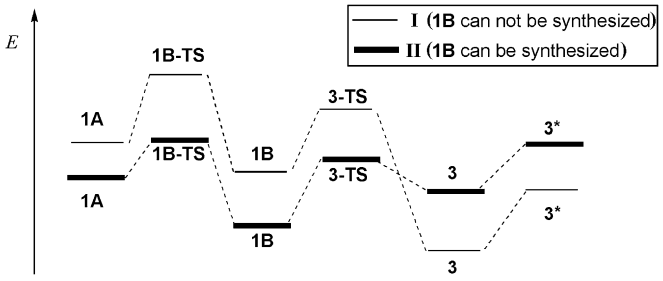

Figure 3. Two putative energy profiles for two alternative cases of the **1A**→**1B**→**3**→**3*** reaction path defined in Scheme 2.

2. Computational methods

Several theoretical methods and a number of basis sets were applied in this study, including HF, DFT(B3LYP),[15] and different high electron-correlation methods. The thermodynamic functions (H, G) were calculated at 298.14 K using the Gaussian03 program[16] at the same levels of theory. For the sake of clarity and simplicity, references to **1A**, **1B**, **3**, and **3*** that have different heteroatoms (Y) and exocyclic substituents on phosphorous (X), are made as **1A(X,Y)**, **1B(X,Y)**, **3(X,Y)**, and **3*(X,Y)**. For a selected family of compounds (X=F and Y=NH, O, S) {**1A(F,Y)**; **1B(F,Y)**; **3(F,Y)**; **3*(F,Y)**} more accurate calculations have also been performed at the BHandHLYP/6-311++G(2d,2p),[17] MP2(FC)/6-311++G(2d,2p),[18] G3MP2,[19] CCSD/6-31++G(d,p),[20] and CCSD(T)/6-311++G(3df,2dp)//CCSD/6-31++G(d,p)[21] levels of theory. Relative energy values of **1A**, **1B** and **3** (ΔE) as compared to **3*** as the reference, computed at the various levels of theory, were plotted against those obtained at the high CCSD(T)/6-311++G(3df,2dp)//CCSD/6-31++G(d,p) level of theory (Tables S1–S6 and Fig. S1). If one considers the CCSD(T) method as the reference method, then the most inaccurate are the HF and MP2, the B3LYP and BHandHLYP methods provide more reliable results, while CCSD and G3MP2 are the best. Finally, a compromise was made between accuracy and economy, and the promising B3LYP/6-311++G(2d,2p) level of theory was used for the present work, where a 4(heteroatom)×12(exocyclic)×6(4minima+2TS)=288 structures were optimized. The optimized enthalpies and Gibbs free energies at 298.14 K were computed with respect to reference structure **3***. (Tables 1 and 2, Tables S1 and S2). Compound **2B** in most cases does not represent a minimum on the potential energy surface. In these cases, the optimized **2B** structures with one imaginary

Table 1
Computed relative and transition states Gibbs free energies (ΔG) for heterophosphetes for X=F, OMe and F indicating relative stabilities

	NH			O			S		
	$\Delta G_{1A\rightarrow 3^*}$	$\Delta G_{1B\rightarrow 3^*}$	$\Delta G_{3\rightarrow 3^*}$	$\Delta G_{1A\rightarrow 3^*}$	$\Delta G_{1B\rightarrow 3^*}$	$\Delta G_{3\rightarrow 3^*}$	$\Delta G_{1A\rightarrow 3^*}$	$\Delta G_{1B\rightarrow 3^*}$	$\Delta G_{3\rightarrow 3^*}$
F	4.2	−15.8	−9.6	30.6	−8.8	−7.7	−5.0	−27.8	—
Cl	26.4	7.0	−4.9	56.3	7.7	−5.6	17.3	−7.6	−4.4
Br	28.3	11.4	−3.4	58.3	—	−4.6	18.3	−5.6	—
CN	4.2	−36.5	—	26.1	−31.1	—	−3.4	−48.9	—
OCN	−25.2	−53.5	—	9.1	−39.4	—	−42.0	−60.6	—
SCN	20.1	−14.8	—	42.7	−3.7	—	4.4	−27.3	—
OMe	78.0	—	−12.0	104.0	—	−15.9	84.3	—	−9.0
NMe$_2$	131.0	—	−11.2	143.3	—	−16.3	138.2	—	−11.4
SMe	84.7	—	4.2	99.2	—	1.9	74.3	—	−1.5
H	62.2	—	−28.4	—	—	−23.2	—	—	−37.7
Me	107.23	—	−24.64	111.68[a]	—	−27.55	—	—	−23.7
Ph[b]	159.27	—	−17.75	—	—	−17.51	—	—	−9.3

[a] **1A** is a stationary point with one imaginary frequency.
[b] Computed at B3LYP/6-31++G(d,p) level of theory.

Table 2
Summary of the computed relative enthalpies for heterophosphetes

X	Y	CH_2	NH	O	S
	F	**1A**>***1B***<**3**<**3***	**1A**>***1B***<**3**<**3***	**1A**>***1B***<**3**<**3***	**1A**>***1B***<**3**<**3***
	Cl, Br	**1A**>**1B**>***3***<**3***	**1A**>**1B**>***3***<**3***	**1A**>**1B**>***3***<**3***	**1A**>**1B**>***3***<**3***
	CN, OCN, SCN	**1A**>***1B***<**3***	**1A**>***1B***<**3***	**1A**>***1B***<**3***	**1A**>***1B***<**3***
	OMe, NMe_2, SMe	**1A**>***3***<**3***	**1A**>***3***<**3***	**1A**>***3***<**3***	**1A**>***3***<**3***
	H, Me, Ph	**1A**>***3***<**3***	**1A**>***3***<**3***	***3***<**3***	***3***<**3***

The italicized number indicate the global minimum of the PES, based on computations carried out at B3LYP/6-311++G(2d,2p) level of theory.

frequency were used in the calculation of ΔH_{H2} values for **1B**→**2B**.

3. Results and discussion

In this section, we discuss the thermodynamic and kinetics aspects of all **1A**, **1B**, and **3** structures containing three different ring heteroatom moieties (Y=NH, O, S) and for 12 exocyclic substituents (X=H, Me, Ph, OMe, NMe_2, SMe, F, Cl, Br, CN, OCN, SCN).

3.1. Thermodynamic aspects

The relative energetics of the four possible structures (**1A**, **1B**, **3**, and **3***) measure thermodynamic stability, while the two transition states **1B**-**TS** (belonging to **1A**→**1B**) and **3**-**TS** (belonging to **1B**→**3**) define kinetic stability. The thermodynamic stability of the **1A** and **1B** species can be measured in two ways. From the synthetic perspective, the Gibbs free energy change of the ring-opening (**1**→**3**) is a critical parameter, which quantifies whether compound **1** undergoes a ring opening or not. In several cases, neither structure of **1**, nor **3** exist. At the same time, **3*** always exists. From the thermodynamics point of view, **3*** can be used as a common reference state and the stabilities of **1A**, **1B**, and **3** can be measured and compared with respect to **3***. Hence, relative values of all thermodynamic functions, including Gibbs free energies were calculated with respect to **3***, implying that $\Delta G(\mathbf{3^*})=\Delta H(\mathbf{3^*})=T\Delta S(\mathbf{3^*})=0.00$ kJ/mol. Compound **3** is expected to exist if both values are exothermic, while compound **1** is expected to be the stable structure if the two values are endothermic. Secondly, by examining the 3×12 3D PESs (six representative PESs are displayed in Fig. 4), one can distinguish three clusters of substituents that may be classified as *Type I* (F, Cl, Br, CN, OCN, SCN), *Type II*/*A* (NMe_2, OMe, SMe), and *Type II*/*B* (H, Me, Ph) substituents. The effect of these clusters differs not only quantitatively, but also in the basic topology of the PESs. The existence of structures **1A**, **1B**, and **3** strongly depends on the type of substituents applied.

(a) Electron-withdrawing groups (EWG) such as halogens, CN, OCN, and SCN belong to *Type I* substituents, which are

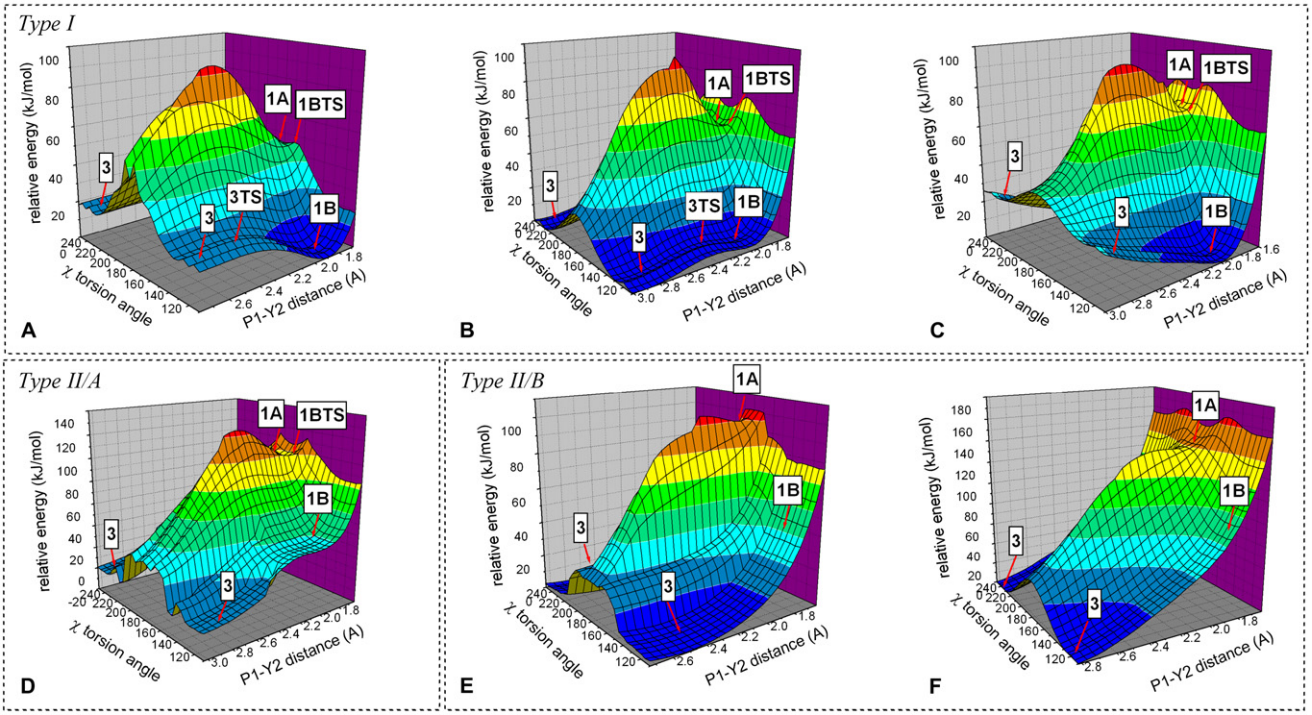

Figure 4. 3D PESs associated with *Type I*: **X**=**F**, Y=**O** (A), **X**=**Cl**, Y=**O** (B), **X**=**Br**, Y=**O** (C), *Type II*/*A*: **X**=**OMe**, Y=**O** (D), *Type II*/*B*: **X**=**H**, Y=**O** (E), **X**=**Me**, Y=**O** (F).

able to stabilize both **1A** and **1B** to occupy distinct energy minima (Fig. 4A–C). The stronger EWGs yield less exothermic and more endothermic ring-opening ΔG values for **1A** and **1B**, respectively. In some cases in the presence of strong EWGs such as CN, OCN, and SCN, the minimum of **3** is annihilated and merges into **1B**, resulting in very stable four-membered rings. As was discussed previously, in all cases, **1A** lies at a higher energy level than **1B**, suggesting that **1B** would be more favorable from the point of view of synthesis (see Tables 1 and 2, as well as Tables S1 and S2). According to thermodynamic stability, structure **1B** with substituents F, CN, OCN may be possible targets for the synthesis of stable heterophosphetes.

(b) The class of *Type II/A* substituents consist of strong electron-donating groups (EDG) and conjugative groups with lone electron pairs on the first atom of X (NMe_2, OMe and SMe). Substituents of *Type II/A* only exhibit **1A**, **3**, and **3*** as a true minima, although the $\Delta G_{\mathbf{1A}\rightarrow\mathbf{3}}$ and $\Delta G_{\mathbf{1A}\rightarrow\mathbf{3}^*}$ values are high and exothermic (>100 kJ/mol). Interestingly, *Type II/A* substituents are unable to stabilize **1B**; therefore, these structures do not represent a stationary point in the downward trend of a PES (Fig. 4D). Instead, around the position of **1B**, the surface is rather flat and horizontal, indicating that this point is almost a stationary point.

(c) Finally, the non-conjugative H, Me, and Ph groups without lone pairs belong to the *Type II/B* substituent class, which destabilizes both **1A** and **1B** heterophosphetes. In the case of these substituents, there are no minima for any of species **1B**, and among **1A** structures, only **1A**(**H**,**NH**) and **1A**(**Me**,**NH**) represent a true minima (Fig. 4E and F); **1A**(**Me**,**O**) lies on a stationary point with one imaginary frequency and is therefore a transition state. In these cases, the ring-opening $\Delta G_{\mathbf{1A}\rightarrow\mathbf{3}}$ and $\Delta G_{\mathbf{1A}\rightarrow\mathbf{3}^*}$ values are also highly exothermic (>100 kJ/mol) (Table 2). It should be mentioned that **1B** is positioned on a completely downward trend of a PES, without any horizontal portions.

For three substituents (Y=F, OMe, Me), ΔG values are summarized for illustrative purposes in Table 1, while all other relevant values are given in Tables S1 and S2. In order to understand how the different types of substituents may influence the topology of the 3D PESs, the antiaromaticity of structures **1A** and **1B** should be investigated.

3.2. Kinetic aspects

The variation of substituents X and heteroatom Y in the heterophosphete results in dramatic changes in the 'reaction profile' (Scheme 2), which is the minimal energy pathway segment (MEP) of the PES (Fig. 4) from **1A** toward **3**. The energy profiles of three different types of substituents (*Type I*, *II/A*, and *II/B*) also show markedly different patterns, and are controlled by the antiaromatic character of **1A** as shown in Figure 5, Table 3 and Table S2. When both **1A** and **1B** exist (*Type I*), these two minima are linked by pseudorotation (Fig. 5A). Pseudorotation may be represented by the dihedral angle χ=X_{axial}–P1–Y2–C3. Thus, χ by definition is 180° for **1A**, and 120° for **1B**, while χ is optimized to 172° in **1B-TS**, as shown in Table 3 and Table S2. The activation Gibbs free energies are rather low ($\Delta G^{\neq}_{\mathbf{1B\text{-}TS}}$ = 3–12 kJ/mol),[6a] which means that the rate of the transformation of **1A** to **1B** is very fast and the $\Delta G^{\neq}_{\mathbf{1B\text{-}TS}}$ value does not depend markedly on the antiaromaticity of **1A**. This low energy TS can be traced to the chemical process (**1A**→**1B-TS**→**1B**), where the antiaromaticity decreases dramatically. The greater stability of **1B** and the low $\Delta G^{\neq}_{\mathbf{1B\text{-}TS}}$ value makes the isolation of **1A** kinetically impossible since the structure of **1B** cannot be frozen with only a 10 kJ/mol barrier height. The energy gap between **1B** and **3** is also rather low ($\Delta G^{\neq}_{\mathbf{3\text{-}TS}} \approx 5-18$ kJ/mol) because of the complete vanishing of remaining weak antiaromatic character. This allows for a fast ring-closing/ring-opening reaction. From the kinetic point of view, it is not possible to trap either **1A** or **1B** if **3** is the thermodynamically preferred structure. However, when **1B** is more stable than **3**, **1B** may be isolated. In the case of substituents of *Type II/A*, **1A** is in fact, a minimum; therefore a low barrier TS appears ($\Delta G^{\neq}_{\mathbf{1B\text{-}TS}} \approx 6-8$ kJ/mol) after **1A**.

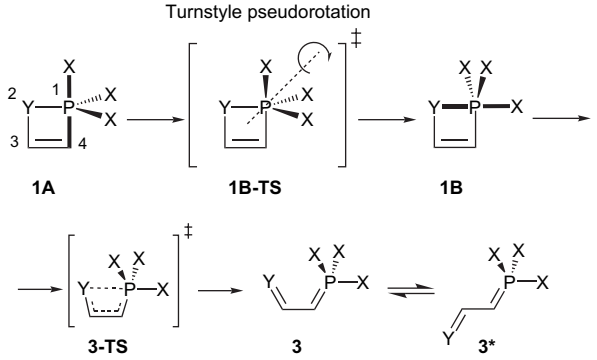

Scheme 2. Reaction mechanism of the transformation of the **1A**→**1B**→**3**→**3*** process.

However, because of the absence of a stable **1B**, the minimum energy pathway (MEP) leads directly to **3** (Fig. 5B). As was mentioned before, in the case of substituents of *Type II/B*, **1A** does not exist for Y=O and S. However, when Y=NH, **1A** is a real minimum with very low stability. The energy profile is therefore very simple (Fig. 5C).

3.3. Antiaromatic character of *1A* and *1B*

The aromaticity/antiaromaticity percentage of compounds **1A** and **1B** with X=F, Cl, CN and Y=O, NH, S were examined earlier,[4] where **1A** was shown to be antiaromatic in contrast to the non-aromatic or slightly antiaromatic **1B** (see Fig. 1). As was shown in Section 3.1, structures **1B** always proved to be more stable than **1A**, namely the energy differences between **1A** and **1B** with Y=O, NH, S, were always negative [ΔH_{pseudo}(**1A**→**1B**)=(−20 kJ/mol)−(−60 kJ/mol)], which was attributed to the annihilation of the antiaromatic character during the pseudorotation process of **1A**→**1B**.[4] However, in the cases of the pseudorotation of non-aromatic **2A** to non-aromatic **2B**, these values proved to be around

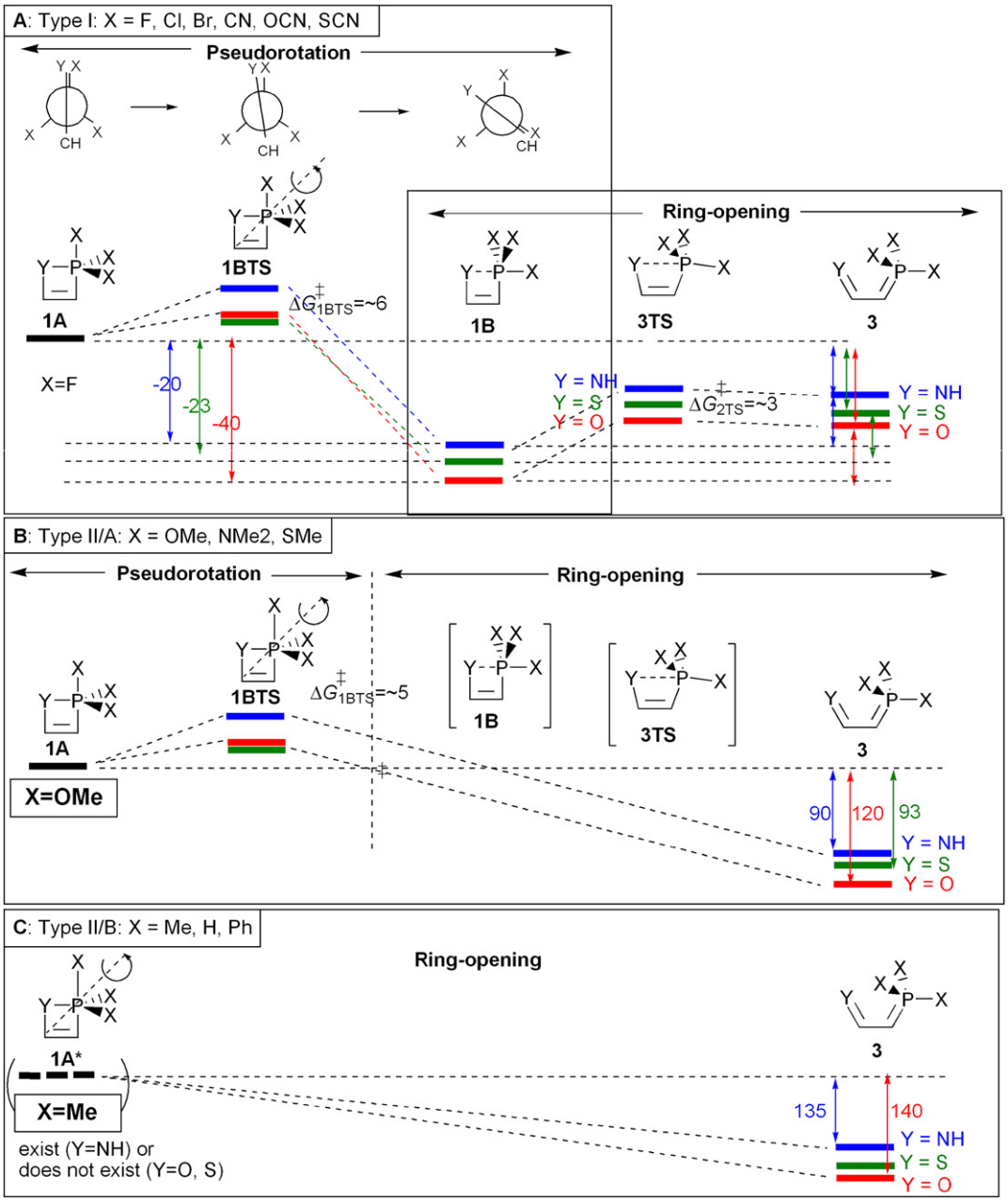

Figure 5. Schematic representations of the energetic profile of the **1A**→**1B**→**3** transformation with different types of substituents denoted by X. The vertical axis is Δ*G* (kJ/mol) and the horizontal axis is the reaction coordinates in arbitrary units.

zero [ΔH_{pseudo}(**2A**→**2B**)=(−6 kJ/mol)−(+2 kJ/mol)]. Analogously to the pseudorotation of **2A**→**2B**, the pseudorotation of **1A**(**X**,**CH$_2$**)→**1B**(**X**,**CH$_2$**) also exhibits relatively small values [ΔH_{pseudo}(**1A**→**1B**)=(−5 kJ/mol)−(−10 kJ/mol)], for the cases when Y=O, NH, S. While **1A**(**X**,**CH$_2$**) and **1B**(**X**,**CH$_2$**) can be considered to be non-aromatic compounds, the large ΔH_{pseudo}(**1A**→**1B**) values for heterophosphetes Y=O, NH, S justify their significant antiaromaticity. Here, we report the antiaromaticity percentage of compounds **1A** and **1B** with 12 exocyclic substituents (X) (Table 4). As was defined earlier, compounds **1**(**X**,**CH$_2$**) are considered to be non-aromatic reference compounds for the calculation of aromaticity percentages. The calculated aromaticity/antiaromaticity data for the 2×3×12 **1A** and **1B** structures summarized in Table 4 reveal two important points. At first (point a), **1A** with exocyclic substituents (X) of *Type II/A* and *Type II/B* exhibits significantly lower antiaromaticity percentages, than **1A** with *Type I* substituents (Fig. 6). Secondly (point b), the question arises why the more antiaromatic **1A** with *Type I* substituents possesses larger thermodynamic stability values (endothermic $\Delta G_{\mathbf{1A}\rightarrow\mathbf{3}^*}$ values) instead of the less antiaromatic **1A** with *Type II/A* and *II/B* substituents.

(a) The less antiaromatic character of **1A** with *Type II/A* and *Type II/B* substituents, X may be attributed to the chemical character of X (Scheme 3). The lone pair on X may result in an ‘exoconjugation’ between X and P1 atom. This

Table 3
Computed activation Gibbs free energies ($\Delta G^{\neq}$, kJ/mol) and key geometric parameters ($\chi_{C3-Y2-P1-xa}$ and r_{P1-Y2} in Å) of selected transition states linking **1A** and **1B**, as well as **1B** and **3**, computed at B3LYP/6-31++G(2d,2p)

	NH				O				S			
	1A→1B-TS		**1B→3-TS**		**1A→1B-TS**		**1B→3-TS**		**1A→1B-TS**		**1B→3-TS**	
	$\Delta G^{\neq}$	$\chi_{C3-O2-P1-Xa}$ (°)	$\Delta G^{\neq}$	r_{P1-O2}	$\Delta G^{\neq}$	$\chi_{C3-S2-P1-Xa}$ (°)	$\Delta G^{\neq}$	r_{P1-S2}	$\Delta G^{\neq}$	$\chi_{C3-N2-P1-Xa}$ (°)	$\Delta G^{\neq}$	r_{P1-N2}
F	7.23	172.6	8.49	2.360	3.60	172.1	5.89	2.448	5.21	167.7	—	—
Cl	9.63	170.9	17.96	2.260	4.26	170.7	14.77	2.211	7.85	165.6	3.66	3.001
Br	10.93	169.7	4.27	2.240	4.63	169.2	—	—	8.98	164.5	—	—
CN	5.48	175.1	—	—	4.98	176.2	—	—	4.57	173.2	—	—
OCN	4.68	175.4	—	—	4.34	175.1	—	—	4.02	173.9	—	—
SCN	4.21	176.2	—	—	4.10	176.4	—	—	3.78	174.1	—	—
OMe	12.34	171.3	—	—	4.57	168.6	—	—	5.91	165.5	—	—
NMe_2	11.25	171.3	—	—	5.10	168.1	—	—	6.18	164.1	—	—
SMe	8.36	171.3	—	—	4.87	169.1	—	—	5.91	165.2	—	—
H	1.66	180.0	—	—	—	—	—	—	—	—	—	—
Me	7.73	171.1	—	—	—	—	—	—	—	—	—	—
Ph[a]	—	—	—	—	—	—	—	—	—	—	—	—

[a] **1A** is a stationary point with one imaginary frequency.

Table 4
Computed aromaticity/antiaromaticity percentages for **1A** and **1B** congeners

Type	X	NH		O		S	
		1A	**1B**	**1A**	**1B**	**1A**	**1B**
I	F	−49.6	−14.3	−40.1	−7.3	−26.8	−4.5
	Cl	−45.1	−6.4	−34.6	5.3	−22.9	6.2
	Br	−42.2	2.5	−31.5	20.6	−20.0	10.2
	CN	−40.3	7.2	−34.1	10.2	−22.5	14.7
	OCN	−57.5	−41.5	−49.6	−20.2	−31.1	−23.7
	SCN	−45.7	−24.8	−52.2	−21.0	−32.1	−12.1
II/A	OMe	−27.3	—	−19.9	—	−30.8	—
	NMe_2	−4.8	—	−3.2	—	1.0	—
	SMe	−17.7	—	−17.9	—	−4.4	—
II/B	H	−20.1	—	—	—	—	—
	Me	−21.5	—	−14.8[a]	—	—	—
	Ph[b]	—	—	—	—	—	—

[a] Stationary point with one imaginary frequencies.
[b] Computed at the B3LYP/6-31++G(d,p) level of theory.

'exoconjugation' competes and decreases the unfavorable internal conjugation between P1 and Y2, and lowers the weight of the antiaromatic resonance structure (**1A-II**). The opposite effect can be recognized in the cases of *Type I* substituents, where the internal conjugation is increased by the strong EWG substituents due to the larger polarization of the P1−Y2 bond, resulting in an increase in the weight of the antiaromatic resonance structure (**1A-II**). This effect is reflected in the P1−Y2 atomic distances, where the shortest bond lengths can be identified in the case of *Type I* substituents (Scheme 3), while in structures **1A** with substituents of *Type II/A* and *Type II/B* the bond distances are significantly longer by 0.06 Å, than in **1A** with substituents of *Type I* (Table S5). It can be also seen that the P1−Y2 bond lengths (*d*) of **1B** are systematically longer by ∼0.05 Å than those of **1A** when both ring structures exist, referring to the larger degree of antiaromaticity of **1A**, than **1B**.

Structural changes as measured by the P1−Y2 bond length (*d*) show direct correlation with the calculated antiaromaticity percentages of **1A** and **1B** (Fig. 6), and are in a good agreement with the hypothesis that shorter P1−Y2 bond lengths increase antiaromaticity. However, in the case of Y=S, the points belonging to **1A** and **1B** represent different lines that are roughly parallel to each other. One may conclude that structure **1B** results in a less antiaromatic ring structure than **1A** due to the different symmetry of the overlapping atomic orbitals on P1 and Y2. This is the first case, when a quantitative relationship was established between antiaromaticity and the bond lengths.

(b) To solve the apparent contradiction of why the less antiaromatic **1A** exhibits increased chemical instability (exothermic $\Delta G_{\mathbf{1A}\rightarrow\mathbf{3}^*}$ value), the whole $\mathbf{1A}\rightleftharpoons\mathbf{3}\rightleftharpoons\mathbf{3}^*$ chemical equilibrium should be taken into consideration (Scheme 4). One may consider the energy level of **1A**(**X**,**Y**) as the zero position. The $\Delta G_{\mathbf{1A}\rightarrow\mathbf{3}}$ and $\Delta G_{\mathbf{1A}\rightarrow\mathbf{3}^*}$ values then reflect the absolute energy levels of **3**(**X**,**Y**) or **3***(**X**,**Y**), and are controlled by the EWG/EDG properties of the X substituents. It was concluded earlier that **1A** with substituents of *Type I* is

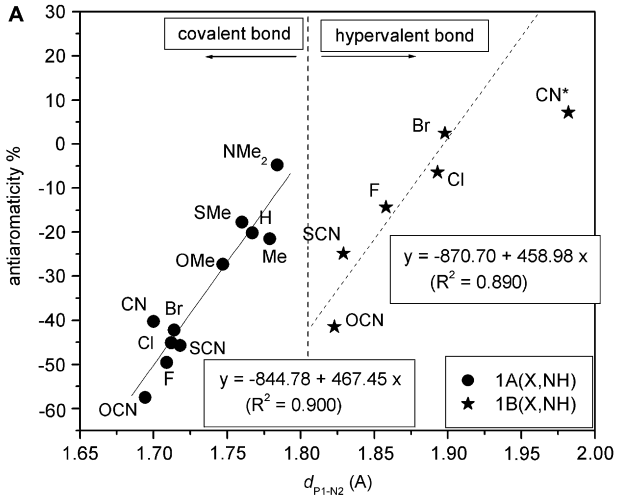

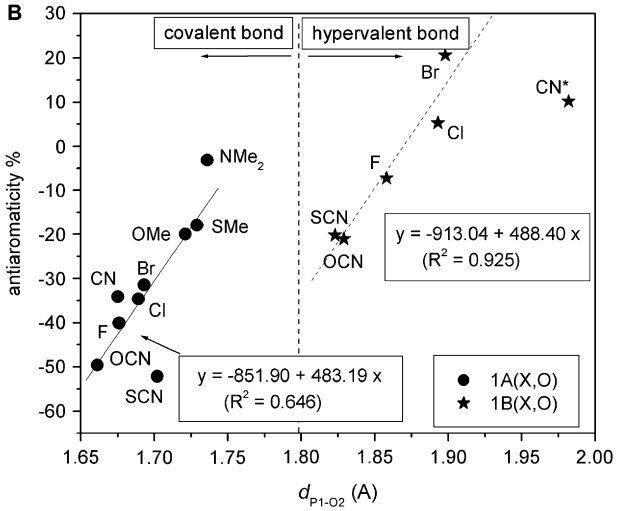

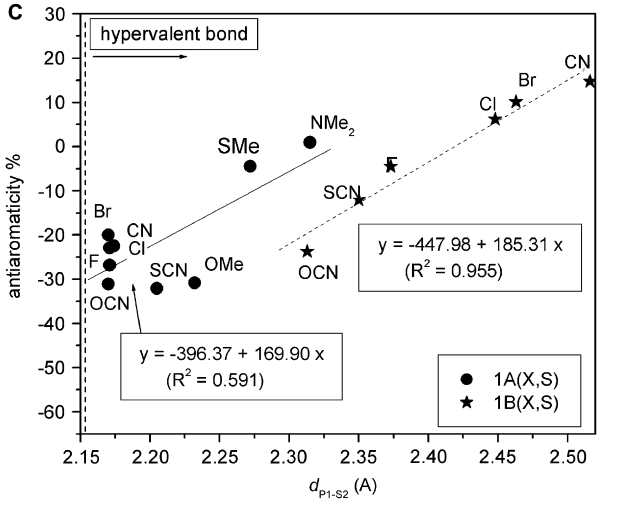

Figure 6. Correlation of ΔG for **1A** and **1B** with the atomic distances of P1–Y2 (r). The points with * (in the case of X=CN) are omitted from the fitting; **A**: Y=NH; **B**: Y=O; **C**: Y=S.

more antiaromatic than **1A** with substituents of *Type II/A*. Therefore, one may conclude that substituents of *Type I* presumably destabilize structure **1A** (Fig. 7). Structures **3**(**X**,**Y**)

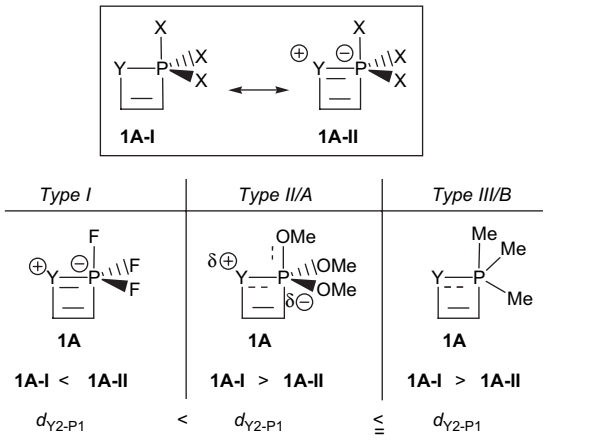

Scheme 3. A schematic illustration of electronic effects exerted by exocyclic substituents (X) of *Types I*, *II/A*, and *II/B*.

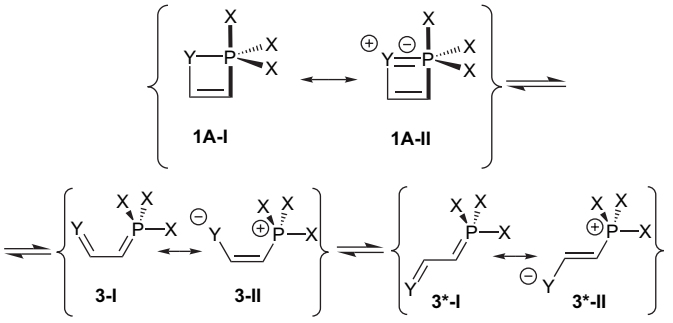

Scheme 4. The equilibrium between **1A**→**3**→**3*** and their most important resonance structures.

and **3***(**X**,**Y**) may be represented by two resonance structures (**3-I**)/(**3*-I**) and (**3-II**)/(**3*-II**) (Scheme 4). The EWG prefers the **3-I**/**3*-I** phosphorane-type resonance structure, while in the case of the EDG, the (**3-II**)/(**3*-II**) ylide-type resonance structure dominates.

Irrespective of X, the Y moiety is electron-withdrawing (NH, O or S) in both cases, and the more conjugated (**3-II**)/(**3*-II**) ylide-type resonance structure represents the more

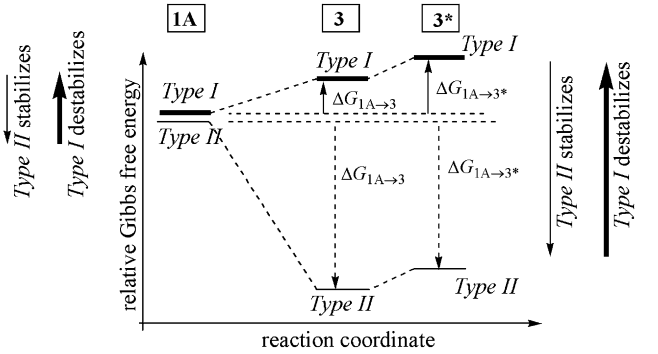

Figure 7. Proposed energy levels for **1A**→**3**→**3*** reactions for substituents of *Type I* and *Type II/A*.

favorable form. This situation is represented by the Natural Bond Orbital (NBO) atomic charges of the Y atom in **3***, as shown in Table 5, where *Type I* substituents exhibits significantly lower negative values, than *Type II/A* and *II/B* substituents, which are close to each other. Due to the delocalization between X and Y through the conjugated X_3–P=C–C=Y backbone, the chemical structure where the ylide-type resonance structure (**3-II**)/(**3*-II**) dominates is more favorable, than resonance structure **3-I/3*-I**. From these data, it can be concluded that electron-donating and conjugative groups of *Type II/A* and non-conjugative *II/B* substituents stabilize, while strong electron-withdrawing groups of *Type I* destabilize structures **3** and **3*** (Fig. 7). This means that electron-donating and conjugative groups of *Type II/A* and non-conjugative groups of *Type II/B* substituents stabilize structures **3** and **3*** to a larger extent than structure **1A**, decreasing the $\Delta G_{\mathbf{1A}\rightarrow\mathbf{3}}$ and $\Delta G_{\mathbf{1A}\rightarrow\mathbf{3}^*}$ values (more exothermic) of this ring-opening reaction (Figs. 7 and 8).

Table 5
Computed NBO atomic charges of the Y atom in **3*** congeners

Type	X/Y	NH	O	S
I	F	−0.664	−0.571	−0.055
	Cl	−0.648	−0.564	−0.049
	CN	−0.622	−0.539	+0.012
II/A	OMe	−0.712	−0.624	−0.173
	NMe_2	−0.721	−0.634	−0.195
	SMe	−0.687	−0.608	−0.144
II/B	H	−0.709	−0.616	−0.156
	Me	−0.734	−0.645	−0.221
	Ph[a]	−0.755	−0.642	−0.221

[a] Computed at B3LYP/6-31++G(d,p) level of theory.

An opposite effect can be recognized for *Type I* substituents. In this case, the *Type I* electron-withdrawing substituents destabilize structures **3** and **3*** to a larger extent than structure **1A**, increasing the $\Delta G_{\mathbf{1A}\rightarrow\mathbf{3}}$ and $\Delta G_{\mathbf{1A}\rightarrow\mathbf{3}^*}$ values (more endothermic) of this ring-opening reaction.

3.4. Substituent effects

The electronic effect (EWG/EDG properties) can be described by the well-known σ_{para}[22] Hammett constant[23] (Fig. 9A–C), which is widely used to measure the reactivity of substituted benzenes.[24] Here we present, as Figure 9A–C indicates, σ_{para} parameters show a relatively good linear correlation with $\Delta G_{\mathbf{1A}\rightarrow\mathbf{3}^*}$ values for Y=NH, O, and S. It is worth mentioning that the slopes of the fitted lines for different Y constituents are almost the same. This may mean that the basic chemical phenomenon is independent from the chemical properties of Y. The different *y*-intercept values are, however, characteristic for Y=NH, O, and S (see the fitted equations in Fig. 9A–C). EWG/EDG properties are usually considered as a combination of the inductive (+I/−I) and a conjugative or resonance (+R/−R) effect[25] (Table 6), with each having clearly different roles. As Table 6 shows, **1A** exists only when the *P*-substituent (X) possesses certain conjugative effects (*Type I* and *Type II/A*), which may decrease the antiaromatic character via external conjugation. The existence of **1B**, requires electron-withdrawing character for *P*-substituents

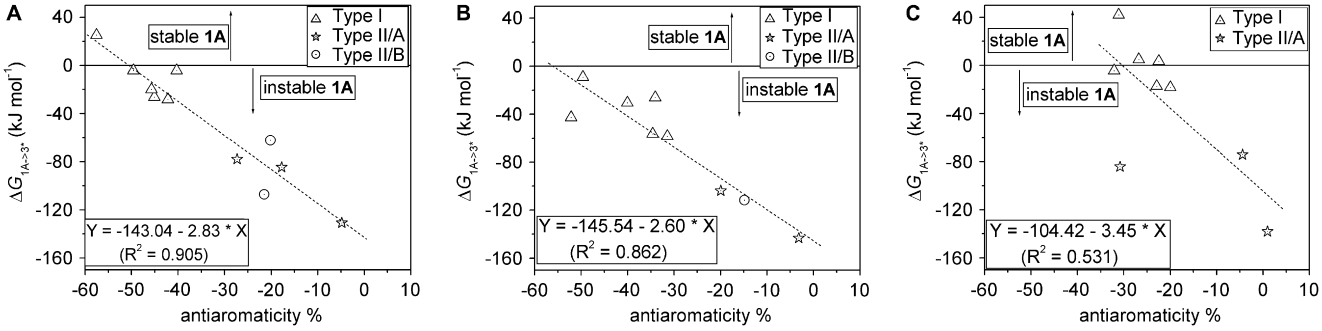

Figure 8. Correlation of thermodynamic stability of **1A** ($\Delta G_{\mathbf{1A}\rightarrow\mathbf{3}^*}$) with calculated percentage aromaticity at the B3LYP/6-311++(2d,2p) level of theory. **A**: Y=NH, **B**: Y=O, **C**: Y=S, **D**: all Y.

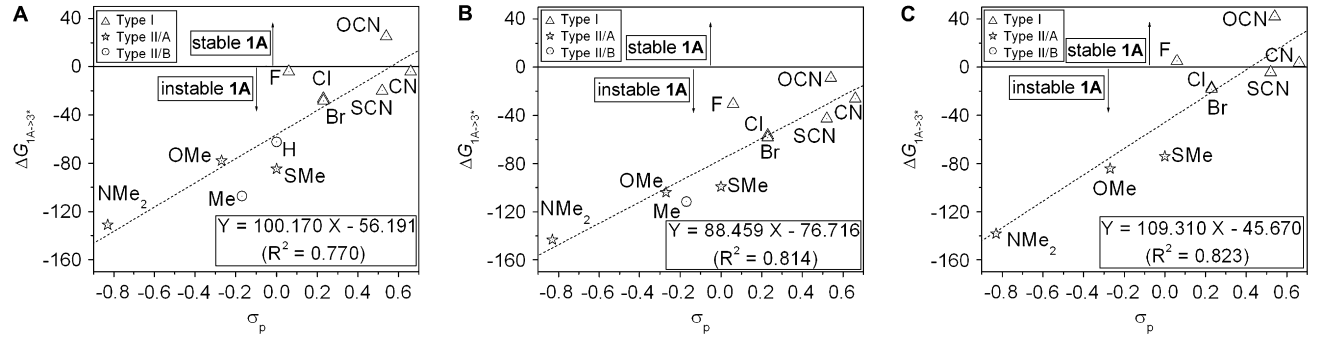

Figure 9. Correlation of $\Delta G_{\mathbf{1A}\rightarrow\mathbf{3}^*}$ values **1A** [B3LYP/6-311++(2d,2p)] with σ_{para} Hammett parameter; **A**: Y=NH, **B**: Y=O, **C**: Y=S.

Table 6
A comparison of various substituents with stability and preferred conformations of simple heterophosphete

	Type I (F, Cl, Br, CN, OCN, SCN	*Type II/A* (OMe, NMe_2, SMe)	*Type II/B* (H, Me, Ph)
Inductive effect	*Strong*	*Medium/weak*	*Weak*
Conjugative effect	*Strong*	*Strong*	*Weak*
Existing structure[a]	**1A**, **1B**, **3**, **3***	**1A**, **3**, **3***	(**1A**), **3**, **3***
Most stable	**1B**	**3**	**3**

[a] With a minimum of the PES.

(*Type I*). The non-conjugative and weakly electron-donating substituents of *Type II/B* cannot stabilize either **1A** or **1B**.

Finally, the percentage of aromaticity/antiaromaticity also shows a relatively good correlation with the σ_{para} Hammett constant. From these data, one may conclude that a stronger EWG causes a larger antiaromaticity percentage.

3.5. Ring strain of heterophosphetes

The ring strain of heterophosphates [**2A**(**Me**,**Y**),**2B**(**Me**,**Y**), where Y=NH, O, S] was determined by isodesmic ring-opening reaction (IR) with C_2H_6 molecule in terms of ΔH_{IR}. Comparing the ΔH_{IR} values obtained for compounds **2** with the similar values of cyclobutane (**7**) and its different congeners (**7**–**11**) one may conclude that while compounds **7**–**11** posses relatively large exothermic values (Scheme 5) that refers to their significant ring strain. At the same time, heterophosphetanes **2** exhibit endothermic values, indicating that these four-membered ring structures are not really strained. The lack of ring strain in **2** can be attributed to the pentavalent P atom, which prefers the rectangular bond angles. As expected, compound **11** containing S atom results in smaller ΔH_{IR} value than those of C, N, and O atoms containing **7**, **9**, and **10** in the same position. However, in the case of non-strained

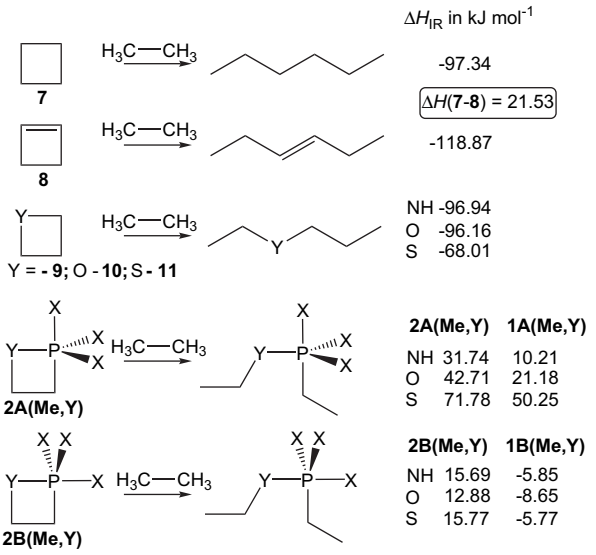

Scheme 5. Isodesmic reaction of **7**–**11** and **2**. Computed enthalpies (ΔH_{IR}, kJ/mol) of the isodesmic reactions of **7**–**11**, **2A** and **2B**, computed at B3LYP/6-311++G(2d,2p); ΔH_{IR}(**1**)=ΔH_{IR}(**2**)−21.53 kJ/mol.

heterophosphetes **2**, the effect of the S atom is already not very significant. The direct determination of ring strains for compounds **1** by isodesmic reaction is not possible, because the calculated ΔH_{IR} values of **1** contains the combination of the ring strain and the antiaromatic stabilization energy. The difference in ΔH_{IR} values computed for **7** and **8** indicates an increased ring strain by the introduction of one double bond into a four-membered ring (21.53 kJ/mol). These data can be considered as an estimation of the ring strain in compounds **1**, subtracting this 21.53 kJ/mol value from ΔH_{IR} values of **2** (Scheme 5). The estimated ΔH_{IR} values of **1** are around zero (Scheme 5), referring that these rings are absolutely non-strained.

4. Conclusion

By studying the electronic effects of three ring heteroatom (Y) and 12 exocyclic substituents (X) on the stability of both conformers (**1A** or **1B**) of heterophosphetes, the following pattern has emerged.

1 The 12 exocyclic substituents studied formed three clusters (*Type I*, *Type II/A*, and *Type II/B*) on the basis of their potential energy surface. Strong electron-withdrawing *P*-substituents (X) (*Type I*) stabilize both **1A** and **1B** ring structures, creating an isolable molecule from synthesis. The electron-donating *P*-substituents of *Type II/A*, as well as non-conjugative *P*-substituents *Type II/B* stabilize the ring-opened structures (**3**); hence, heterophosphetes with these substituents are not a good target for synthesis.
2 The complete energy profile of the **1A**→**1B**→**3**→**3*** reaction sequences were studied for 12 X substituents and three heteroatoms, revealing the overall thermodynamic and kinetic consequences. Due the fact that all TSs are low, therefore all reaction steps are comparably fast (the kinetic stability is low), consequently the thermodynamic stability may control and determine the stability of forming products.
3 There is a virtual contradiction where the more antiaromatic **1A** has larger thermodynamic stability. This could be solved by the detailed study of the whole equilibrium of **1A**⇌**1B**⇌**3**⇌**3***.
4 The electron-donating/withdrawing and conjugating effects of exocyclic substituents (X) can be quantified by the Hammett σ_{para} constant.

Acknowledgements

The authors acknowledge the support from the Hungarian Scientific Research Fund (OTKA T67679), and thank Suzanne K. Lau for her assistance in the preparation of this manuscript.

Supplementary data

The full author list for Ref. 16. Tables S1–S6 contains the computed energies (E), zero-point energies (E_{ZPE}), internal

energies (U) and enthalpies (H) in Hartree at various levels of theories for compounds **1**–**3***. A more detailed method section with Figure S1. *XYZ* coordinates of all compounds. Supplementary data associated with this article can be found in the online version, at doi:10.1016/j.tet.2007.11.094.

References and notes

1. (a) De Proft, F.; Geerlings, P. *Chem. Rev.* **2001**, *101*, 1451–1464 and references therein; (b) Maier, G. *Angew. Chem., Int. Ed. Engl.* **1974**, *13*, 425–490 and references therein; (c) Fattahi, A.; Lis, L.; Tian, Z.; Kass, S. R. *Angew. Chem., Int. Ed.* **2006**, *45*, 4984–4988.
2. (a) Fattahi, A.; Lis, L.; Kass, S. R. *J. Am. Chem. Soc.* **2005**, *127*, 3076–3089; (b) Minkin, V. I.; Glukhotsev, M. N.; Simkin, B. Y. *Aromaticity and Antiaromaticity: Electronic and Structural Aspects*; Wiley: New York, NY, 1994; (c) Maier, G. *Angew. Chem., Int. Ed. Engl.* **1988**, *27*, 309–332 and references therein.
3. Mucsi, Z.; Keglevich, G. *Eur. J. Org. Chem.* **2007**, 4765–4771.
4. Mucsi, Z.; Körtvélyesi, T.; Viskolcz, B.; Csizmadia, I. G.; Novák, T.; Keglevich, G. *Eur. J. Org. Chem.* **2007**, 1759–1767.
5. (a) Keglevich, G.; Forintos, H.; Körtvélyesi, T. *Curr. Org. Chem.* **2004**, *8*, 1245–1261; (b) Keglevich, G.; Körtvélyesi, T.; Forintos, H.; Lovas, S. *J. Chem. Soc., Perkin Trans. 2* **2002**, 1645–1646; (c) Keglevich, G.; Forintos, H.; Körtvélyesi, T.; Tőke, L. *J. Chem. Soc., Perkin Trans. 1* **2001**, 1–3; (d) Keglevich, G.; Körtvélyesi, T.; Forintos, H.; Vaskó, Á.-Gy.; Vladiszlav, I.; Tőke, L. *Tetrahedron* **2002**, *58*, 3721–3727; (e) Keglevich, G.; Dudás, E.; Sipos, M.; Lengyel, D.; Ludányi, K. *Synthesis* **2006**, *8*, 1365–1369.
6. (a) Vansteenkiste, P.; van Speybroeck, V.; Verniest, G.; De Kimpe, N.; Waroquier, M. *J. Phys. Chem.* **2007**, *111*, 2797–2803; (b) Altman, J. A.; Yates, K.; Csizmadia, I. G. *J. Am. Chem. Soc.* **1976**, *98*, 1450–1454.
7. Smith, D. J. H. *Comprehensive Organic Chemistry*; Barton, D., Ed.; Pergamon: Oxford, 1979; Vol. 2, Chapter 10.4, pp 1233–1256.
8. Kano, N.; Kikuchi, A.; Kawashima, T. *Chem. Commun.* **2001**, 2096–2097.
9. Kawashima, T.; Iijima, T.; Kikuchi, A.; Okazaki, R. *Phosphorus, Sulfur, Silicon Relat. Elem.* **1999**, 144–146 and 149–152.
10. (a) Poater, J.; Duran, M.; Solà, M.; Silvi, B. *Chem. Rev.* **2005**, *105*, 3911–3947; (b) Krygowski, T. M.; Stępień, B. T. *Chem. Rev.* **2005**, *105*, 3482–3512.
11. Schleyer, P. v. R.; Maerker, C.; Dransfeld, A.; Jiao, H.; Hommes, N. J. R. v. E. *J. Am. Chem. Soc.* **1996**, *118*, 6317–6318.
12. Chen, Z.; Wannere, C. S.; Corminboeuf, C.; Puchta, R.; Schleyer, P. v. R. *Chem. Rev.* **2005**, *105*, 3842–3888.
13. (a) Krygowski, T. M.; Ejsmont, K.; Stępień, B. T.; Cyrański, M. K.; Poater, J.; Solà, M. J. *J. Org. Chem.* **2004**, *69*, 6634–6640; (b) Cyrański, M. K.; Schleyer, P. v. R.; Krygowski, T. M.; Jiao, H. J.; Hohlneicher, G. *Tetrahedron* **2003**, *59*, 1657–1664.
14. Mucsi, Z.; Viskolcz, B.; Csizmadia, I. G. *J. Phys. Chem. A.* **2007**, *111*, 1123–1132.
15. (a) Stephens, P. J.; Devlin, F. J.; Chabalowski, C. F.; Frisch, M. J. *J. Phys. Chem.* **1994**, *98*, 11623–11627; (b) Beke, A. D. *J. Chem. Phys.* **1993**, *98*, 5648–5651.
16. Frisch, M. J.; Trucks, G. W.; Schlegel, H. B.; Scuseria, G. E.; Robb, M. A.; Cheeseman, J. R.; Zakrzewski, V. G.; Montgomery, J. A.; Stratmann, R. E., Jr.; Burant, J. C.; Dapprich, S.; Millam, J. M.; Daniels, A. D.; Kudin, K. N.; Strain, M. C.; Farkas, O.; Tomasi, J.; Barone, V.; Cossi, M.; Cammi, R.; Mennucci, B.; Pomelli, C.; Adamo, C.; Clifford, S.; Ochterski, J.; Petersson, G. A.; Ayala, P. Y.; Cui, Q.; Morokuma, K.; Malick, D. K.; Rabuck, A. D.; Raghavachari, K.; Foresman, J. B.; Cioslowski, J.; Ortiz, J. V.; Baboul, A. G.; Stefanov, B. B.; Liu, G.; Liashenko, A.; Piskorz, P.; Komaromi, I.; Gomperts, R.; Martin, R. L.; Fox, D. J.; Keith, T.; Al-Laham, M. A.; Peng, C. Y.; Nanayakkara, A.; Challacombe, M.; Gill, P. M. W.; Johnson, B.; Chen, W.; Wong, M. W.; Andres, J. L.; Gonzalez, C.; Head-Gordon, M.; Replogle, E. S.; Pople, J. A. *Gaussian 03 6.0*; Gaussian: Pittsburgh, PA, 2003.
17. Note that BHandHLYP means $0.5\times E_X^{HF}+0.5\times E_X^{LSDA}+0.5\times \Delta E_X^{Becke88}+E_C^{LYP}$functional.
18. Head-Gordon, M.; Pople, J. A.; Frisch, M. J. *Chem. Phys. Lett.* **1988**, *153*, 503–505.
19. Curtiss, L. A.; Raghavachari, K.; Pople, J. A. *J. Chem. Phys.* **1993**, *98*, 1293–1298.
20. Purvis, G. D.; Bartlett, R. J. *J. Chem. Phys.* **1982**, *76*, 1910.
21. Pople, J. A.; Head-Gordon, M.; Raghavachari, K. J. *Chem. Phys.* **1987**, *87*, 5968–5972.
22. Hansch, C.; Leo, A.; Taft, R. W. *Chem. Rev.* **1991**, *91*, 165–195.
23. (a) Hammett, L. P. *J. Am. Chem. Soc.* **1937**, *59*, 96–103; (b) Hammett, L. P. *Physical Organic Chemistry*, 2nd ed.; McGraw-Hill: New York, NY, 1970; pp 347–390.
24. (a) Wells, P. R. *Linear Free Energy Relationships*; Academic: New York, NY, 1968; (b) Wells, P. R. *Chem. Rev.* **1963**, *63*, 171–219; (c) Johnson, C. D. *The Hammett Equation*; Cambridge University Press: Cambridge, 1973.
25. (a) Ehrenson, S.; Brownlee, R. T. C.; Taft, R. W. *Prog. Phys. Org. Chem.* **1973**, *10*, 1–16; (b) Taft, R. W.; Topsom, R. D. *Prog. Phys. Org. Chem.* **1987**, *16*, 1–16.